Melting behaviour of waste glass cullet briquettes in soda-lime-silica container glass batch

DENG, Wei, WRIGHT, Richard, BODEN-HOOK, Chris and BINGHAM, Paul <http://orcid.org/0000-0001-6017-0798>

Published version

DENG, Wei, WRIGHT, Richard, BODEN-HOOK, Chris and BINGHAM, Paul (2019). Melting behaviour of waste glass cullet briquettes in soda-lime-silica container glass batch. International Journal of Applied Glass Science, 10 (1), 125-137.

Melting Behaviour of Waste Glass Cullet Briquettes in Soda-Lime-Silica Container Glass Batch

Wei Deng [a,2], Richard Wright [b], Chris Boden-Hook [b] and Paul A Bingham [a,1]

[a.] Materials and Engineering Research Institute, Faculty of Arts, Computing, Engineering and Sciences, Sheffield Hallam University, City Campus, Howard Street, Sheffield S1 1WB, UK

[b.] Wright Engineering Ltd, Blyth Road, Worksop S81 8BP, UK

Abstract

The melting behaviour of representative container glass batch with and without the addition of 15wt % briquettes produced from waste cullet fine particles was investigated in the context of reducing both waste and glass melting energies. Carbonate raw material decomposition and reactions during melting were studied by DTA-TGA-MS. The decomposition kinetics of two batches, representing typical container glass batches with 0% and 15% briquette additions, were calculated by transformation degree based on the Ginstling-Brounstein and Arrhenius equations. High temperature phase transitions and fractions of silica reaction in each batch were obtained from X-ray diffractometry (XRD). The briquette additions accelerated the decomposition reactions and the silicate reaction kinetics by decreasing the activation energy for carbonate decomposition. Silica sand in the batch was shown to melt at lower temperatures with the addition of briquettes. Batch melting processes at different temperatures and briquette melting on top of the molten glass at high

[1] Corresponding author, email p.a.bingham@shu.ac.uk
[2] First author, email wei.deng@shu.ac.uk, dengwei19@gmail.com

temperatures, were investigated by macroscopic investigations of sample cross-sections post-melting. The positive effects of briquette additions to container glass batches, in terms of increased melting rate and reduced batch reaction and decomposition temperatures, are supported by the results of this study.

Keywords: glass; cullet; energy; melting; briquette; consolidation

1. Introduction

In modern soda-lime-silica type container glass manufacturing, large amounts of waste glass or cullet are recycled and remelted as glass batch constituents, reducing melting energy and fuel consumption, and thereby reducing CO_2 emissions[1][2][3][4]. In the UK, about 640,000 tonnes of glass packaging waste were recycled in the first three quarters of 2017 according to UK Government's National Packaging Waste Database. In many Western European glass plants, the introduction of 80% or more of recycled cullet for the melting of green container glass is common practice [1]. Cullet can act as a fluxing agent and decreases glass melting energies. Compared with virgin (mined and man-made) glass batch raw materials, the melting energy consumption of cullet is approximately 70-75% [5]. However, approximately 20 wt% of all recycled cullet has too small a particle size (i.e. is too fine) to be safely re-introduced into glass melting furnaces without increasing the likelihood of problems associated with bubbles, foaming and refining. Consequently, up to 20 wt % of all recycled cullet is currently land filled as a waste. To extend and secure glass batch sources, by recycling cullet fines and alleviating uptake of landfill facilities (of

which there are shortages), a primary study of the recycling of cullet fines through briquetting and re-introduction into representative container glass batches and products, and its effects therein, has been described recently by the present authors [6]. Briquettes consisting of 82 wt % recycled cullet fines were made with additions of sodium silicate, sodium carbonate and water. The compressive strength of briquettes was shown to increase linearly with time, increasing from 2 MPa to 60-65 MPa after 33 days at room temperature (ca. 20^{o}C) and ambient humidity [6]. With compensation of the other glass batch materials to maintain a consistent nominal final glass composition, it was demonstrated that up to 15 wt % briquettes could be added to a representative green container glass batch, and produce glasses with comparable compositions and properties to glasses produced using briquette-free batches, supporting the potential use of this technology for enhanced energy and resource efficiency, and lower CO_2 emissions, from commercial glass manufacture through increased cullet usage.

Melting behaviour of glass batches with briquette additions is also attracting attention in the context of lower energy consumption (hence fuel use and CO_2 emissions). Modifications of batch materials, in terms of particle size, distribution and proportion of batch ingredients, leads to differences in specific melting energy. According to Beerkens [7], energy consumption distribution during glass melting in commercial furnaces is highly uneven. Approximately 75 - 90 % of total theoretical heat needed for melting is absorbed by the batch during the first 0.75-1h to heat the batch material to 1200-1250^{o}C. Energy consumption is intensive in the first stage of

glass melting but only 5 % of the total heat transfer time is involved in this step.

The theoretical sand grain dissolution time for soda-lime-silica glass melts is ~1.5 - 2 h at 1300 - 1350^{o}C; the removal of gas bubbles requires a minimum 2 - 3 h in the fining zone; and the theoretical homogenization time of the melt by stirrers is ~0.5h [7]. In reality, the residence time of molten glass in commercial furnaces is even longer (24 - 60 hours for the first molten glass circuit around the furnace backflow before the hot point in cross-fired furnaces) [8]. Depending on the type and capabilities of the furnace, more than 40 % total energy can be consumed to keep the molten glass temperature constant during these stages (sensible heat). Evaluating the energy consumption of glass batch melting is thus highly complex. It not only involves the endothermic fusion and carbonate decomposition energy requirements for transforming the batch into molten glass [9], but also the energy for melting and manufacturing processes such as sand dissolution, bubble removal and glass melt homogenization.

A classical method, consisting of cross-sections of crucibles containing batches at different stage of melting, has been widely used to observe the melting behaviour of glass batches on a laboratory scale. In 1969, Bunting and Bieler [10][11] published research on melting and batch-free times using this method. Sections of crucibles containing melted cullet with batches melted in different conditions were surveyed by orthoptic observation. To investigate the glass melting reactions over a wide range, Dolan and Misture [12-14] carried out comprehensive studies on (i) 18 different industrial glass batch component reactions [12]; (ii) binary and ternary quartz-sodium

carbonate-calcium carbonate batches, with and without cullet reactions [13]; and (iii) quartz-calcium carbonate-alumina-borate batch with and without cullet reaction [14] by in-situ XRD. Different phase transition paths were found and investigated in detail [12-14]. Within the limits of their studies, Dolan and Misture noticed that the phase transitions of binary and ternary soda-lime-silica glass batches during heating are dependent not only on the overall composition, but also on particle–particle interactions. Cullet did affect the amounts of each phase formed and the rate of formation [13]. Thermal analysis has also been used to identify each glass melting reaction in complex glass batch systems. Hong and Speyer [15][16] investigated one-component systems of feldspar, sand, soda ash, calcite, dolomite, and other additives in binary, ternary and multicomponent systems by differential thermal analysis (DTA). Reactions in soda-lime silica glass batches containing different additions, such as Na_2SO_4, $NaNO_3$, NaCl, were studied and the effects of additives on reaction rates were illustrated. However, it can be difficult to interpret kinetic effects through thermal analysis. To determine carbonate decomposition rates during glass batch reactions, Cheng *et al*. [17] carried out kinetic calculations based on thermal mass loss of original non-milled glass batch. The effects of granulation of the raw materials (increasing low thermal conductivity of loose batch, which limits the melting rate of glass and pull rate of the furnace) and heating them before introduction into the furnace were investigated by DTA, XRD and carbonate decomposition kinetic analysis based on the theory of the Ginstling-Brownstein and Arrhenius equations. Their calculations indicated that the activation energy for decomposition of

carbonate in granulated batch is lower than that of loose batch: granulation promoted the decomposition of carbonate raw materials during melting and the activation energy decreased with increasing binder (carboxyl methyl cellulose) solution concentration. Few investigations have been carried out on the melting behaviour of briquetted glass raw materials and, to our knowledge, none had previously studied briquetted glass fines prior to our recent study [6].

In this paper, we build on our previous work [6] to study the melting behaviour, rates and kinetics of a representative commercial green container glass batch and compare and contrast it with a modified batch containing 15 wt. % briquettes. The decomposition of carbonates; melting of quartz and other components; and fusion and melting during heating were studied by XRD. Differential thermal analysis / thermogravimetry coupled to a mass spectrometer (DTA/TGA-MS) was used to determine the thermal properties, weight loss and gas release from the batch during heating. The reaction rates of carbonate decomposition were determined by weight loss from original glass batch at different temperatures. Finally, sections of crucibles containing batches heated for different times (stages-of-melting survey) were used to observe the melting processes of the different batches.

2. Experimental Procedures

Briquettes were manufactured by mixing sodium silicate, sodium carbonate, glass fines and water, as described in [6]. Briquettes were produced using a proprietary mechanical method which consistently produced briquettes of typical dimensions 20 x

30 x 40 mm. After thorough mixing of the briquette constituents, the mixture was fed into a roller press with moulds on a double roll to compress the mixture into a briquette at applied pressures of ca. 50 MPa. After formation, briquettes were passed along a conveyor belt with heating to partially dry them at around 80^{o}C for 2 minutes, then collected and stored in polyethylene bags in air.

The representative (benchmark) green container glass batch (Batch A) and a modified batch (Batch B-15) containing 15 wt% briquettes were melted under laboratory conditions and these two batch compositions are given in Table 1. Batch B-15 was produced, wherein briquettes partially replaced standard cullet at 15 wt. %, with proportional modification of other batch constituents to provide the same nominal final glass composition as the benchmark glass. Industrial glass making raw materials and cullet were kindly provided by a UK container glass manufacturer, and raw materials were dried at 110^{o}C for a minimum of 24 hours.

Batches were weighed out using a 4-decimal place balance to provide batches weighing 200g. Batches were thoroughly mixed and were then placed in recrystallized Al_2O_3 crucibles. Crucibles were heated in an electric furnace at a rate of 4^{o}C / minute to 1450^{o}C and then held at this temperature for 4h. Crucibles were then removed from the furnace and the molten glass poured into a stainless steel mould and allowed to cool until sufficiently rigid to remove the mould. The glass was then annealed at 520^{o}C for 1h, then cooled slowly to room temperature. Resulting glass compositions were determined using X-ray fluorescence spectroscopy (wavelength dispersive Philips PW2440 sequential X-ray fluorescence spectrometer) and the results are

presented in Table 2. Uncertainties associated with the XRF analyses are estimated at ±2% of measured concentrations.

After thoroughly mixing and milling, benchmark Batch A and modified glass Batch B-15 were characterized by differential thermal analysis/thermogravimetry (Netzsch STA 409PG Luxx®) coupled to an Aëolos spectrometry analysis (DTA / TGA–MS) using heating rates of 5 K/min from 22^{o}C to 1400^{o}C.

To determine the phase transition of glass batch during heat treatment, batches to produce 100g of glass were weighed out by using a 4-decimal place balance. Several batches of each type were weighed and thoroughly mixed; and were then placed in recrystallized Al_2O_3 crucibles. The crucibles were heated in an electric furnace at a rate of 5^{o}C / minute to 900^{o}C, 1000^{o}C, 1100^{o}C, 1200^{o}C or 1300^{o}C and then removed from the furnace and cooled to room temperature in air, in order to survey melting reactions over different temperature ranges. The product materials were carefully removed from the crucibles then crushed and sieved through a 74 μm (200-mesh) sieve. X-ray diffraction (XRD) was carried out on each sample using a Panalytical X'Pert Pro X-Ray Diffractometer. Measurements were taken from diffraction angles (2θ) between 10^{o} and 90^{o} at a rate of 0.02^{o} per second. Phase identification was performed using Jade software and ICDD powder diffraction files (International Center for Diffraction Data).

To determine the reaction degree of carbonate decomposition in batches during heat treatment, a loss on ignition experiment was carried out. Batch A and Batch B-15 were weighed out to 40 g by using a 4-decimal place balance, thoroughly mixed, and

placed into recrystallized Al_2O_3 crucibles. In order to reduce errors brought by any weight loss from crucibles, the crucibles had already been heated at 850 °C for several hours and self-cooled in a dryer. All crucibles were then heated at 200 ^oC for 6h to eliminate any errors that could arise due to moisture in the crucible or batch materials therein. Four Al_2O_3 crucibles containing dried batches were then placed in an electric furnace at different temperatures (675, 700, 725, 750 °C) and treated for different holding times (0, 15, 30, 45 and 60 min). The crucibles were removed from the furnace and weighed every 15 mins.

To observe the reaction behaviour of the batch during melting, a "stages of melting" survey, which consisted of cutting cooled crucibles containing the reaction products in half, was carried out on Batch A and Batch B-15 samples, to reveal the resulting macrostructure of the reacted batch materials. Here, seven batches were weighed (40g each) and placed in Al_2O_3 crucibles (internal opening diameter: 30mm; height of crucible: 50mm). and placed in an electric furnace. Crucibles were heated at a rate of 4^oC / min to 1000^oC, 1100^oC, 1200^oC, 1300^oC, 1450^oC and 1450^oC and held at these temperatures for 1h. The crucibles were then removed from the furnace and annealed in another electric furnace at 520^oC for 1h, then cooled slowly to room temperature. To compare the melting behaviour of Batch A and Batch B-15 as functions of temperature and time, crucibles were cut down their central axis using a diamond saw. Some crucibles were sealed in epoxy resin prior to cutting, in order to prevent cracking and spalling during cutting. These half crucibles were compared to one another allowing visual assessments of melting behaviour to be made.

In order to directly observe the melting behaviour and melting rates of briquettes, briquettes were cut into cubes (20mm×10mm×10mm). Nine Batch A batches were placed into Al_2O_3 crucibles and heated at a rate of 5^{o}C / min to 1450^{o}C/4h in an electric furnace, then each crucible was removed from the furnace, and a briquette cube was placed on the top of molten glass in each crucible. Each crucible was quickly returned to the furnace and heated at the same temperature, 1450^{o}C. Different crucibles were heated for different times from 10 s to 10 min) with each removed from the furnace after the appropriate time and annealed in an electric furnace at 520^{o}C for 1h, then slowly cooled to room temperature. These crucibles were the cut down their central axis by a diamond saw, and some crucibles were sealed with epoxy resin to prevent cracking or spalling during cutting. These half crucibles were compared to one another allowing a visual estimate of melting behaviour and melting rates to be made.

3. Results

3.1 Batch composition

Owing to the presence of binder materials (sodium silicate and sodium carbonate) in the briquettes, and in order to keep the final target glass composition unchanged from that of the benchmark glass, Batch B-15 was modified. This largely consisted of reducing the sand and sodium carbonate contents of Batch B-15 compared with Batch A. XRF analyses of final glasses are also shown in Table 2, which were also included in our previous work describing briquette additions to SLS container glass batches[6].

The XRF results confirm, within experimental uncertainties, that the chemical composition of the benchmark glass Batch A was essentially maintained for Batch B-15 glass.

These two representative glass batches were carefully selected to enable direct comparison in this study. Batch B-15 is a modification based on Batch A through the introduction of briquettes, and Batch A is broadly representative of current industrial green container glass batches. The high batch content of cullet (87 wt.%) and low content of virgin mined and man-made glass batch raw materials present a very high standard of practical technology in the glass industry. Not only the high content of cullet and the minor carbonate and sand usage can save energy and reduce CO_2 emissions,[18] but also the recycling of filter dust and wastes can further reduce costs and environmental impact.

3.2 X-Ray Diffractometry (XRD)

The reacted Batch A and Batch B-15 samples, heated to different temperatures, were analysed using XRD. Figure 1 a. and b. present the sequences of XRD patterns for Batch A and Batch B-15 before heating to 900^{o}C, 1000^{o}C, 1100^{o}C, 1200^{o}C and 1300^{o}C. For the as-mixed (unheated) Batch A and Batch B-15, the XRD patterns are almost identical, with quartz (SiO_2, PDF# 05-0490) and dolomite ($CaMg(CO_3)_2$, PDF# 05-0522) phases identified. Following heat treatment at 900^{o}C, the dolomite phase had disappeared from both Batch A and Batch B-15, and a complex low-symmetry phase $Na_4Ca_4(Si_6O_{18})$ (PDF# 75-1686) was observed only in Batch A.

Meanwhile, formation of the high temperature phase wollastonite ($CaSiO_3$, PDF# 03-0626) in both Batch A and Batch B-15 was identified through the reflection at $2\theta=29.96^o$. At 1000^oC, the relative intensity of reflections corresponding to the wollastonite in Batch A and Batch B-15 increases, indicating increasing formation between 900^oC and 1000^oC. The relative peak intensity from quartz decreases with increasing temperature for both batches, consistent with dissolution of sand grains in the surrounding liquid. From 1100^oC to 1300^oC, the only crystalline phase present was quartz, with the relative peak intensity at $2\theta=26.74^o$ decreasing with increasing temperature. The $2\theta=26.74^o$ quartz peak had disappeared at 1200^oC and 1300^oC for Batch A and Batch B-15, respectively.

3.3 DTA-TGA-MS

The thermal analysis (DTA-TGA) coupled with Mass Spectroscopy (MS) data for Batch A and Batch B-15, at a heating rate of 5^oC/min, are shown in Fig. 2. From the TGA curves and mass spectra, it is confirmed that mass loss up to 100^oC is caused by the loss of water. The mass loss between ca. 300^oC and 700^oC is attributed to the decomposition of carbonate raw materials and corresponding gaseous release of CO_2. Two stages of carbonate decomposition can be clearly observed from the mass loss of CO_2 as shown. The first CO_2 ion density peak in the Batch A graph, peaking at ca. 550^oC, is less intense than that of the second CO_2 ion density peak at ca. 680^oC. On the contrary, the CO_2 ion density peak of Batch B-15 at ca. 550^oC is more intense than that at ca. 680^oC. To enable comparison and eliminate the effects of water evaporation,

the normalized TGA curves of Batch A and Batch B-15 from 300^{o}C to 800^{o}C are presented in Fig.3.

The CO_2 release from Batch B-15 demonstrably occurs at lower temperatures than that from Batch A, and the carbonate decomposition of Batch A and Batch B-15 is completed at 700^{o}C and 660^{o}C, respectively. The DTA curves for Batch A and Batch B-15 do not show obvious exothermic peaks or endothermic troughs during the decomposition of carbonates. Meanwhile, the major reactions of a more than three component system occur in the short temperature range of 700^{o}C - 900^{o}C[19][20]. It is challenging to unambiguously interpret the results of thermal analysis in such complex systems [15]. A potential way to identify individual reactions is by comparison of the results with those of simple binary mixtures. Traditional glass batch components such as sand, dolomite and sodium carbonate are chemically independent and can provide clear thermal signals for carbonate decomposition or other chemical reactions between themselves during batch melting. Although more than 85% of the batch is cullet or glass fines in our research, the reactions that are caused by these components may still be used to identify (or at least reference) the degree of glass batch melting through the weak thermal signals (exothermic peaks or endothermic troughs) in the DTA trace.

For binary components, Hong and Speyer carried out thermal analysis on feldspar-soda ash, silica-soda ash, dolomite-soda ash and silica-dolomite by DTA and TGA.[15] The main endothermic troughs for these binary mixtures are ranged from 800^{o}C to 900^{o}C with the TGA curve indicating mass loss (decomposition of

carbonate), except for silica-dolomite. For silica-dolomite, the large heat capacity of quartz tended to broaden and lower the intensity of the dolomite decomposition peak and make the trough barely perceptible. Through the TGA and mass spectroscopy in this research, the decomposition of carbonate was observed from 400^{o}C to 700^{o}C without an endothermic trough from DTA. On one hand, such a low decomposition range could be attributable to the accelerating effects of cullet[21]. On the other hand, the decomposition endothermic DTA signal should be broadened and neutralized by the large heat capacity of the very high cullet content. The weak endothermic troughs that were found from 700 to 900^{o}C for Batch A and Batch B-15 should be caused by other complex chemical reactions between polysilicates in crystalline or non-crystalline form. Such complex thermal behaviour is not only caused by the complex composition of the glass batch, but also the very high cullet content.

3.4 Weight Loss from Original Batches

Data showing the degree of transformation of Batch A and Batch B-15, when heating over the temperature range 675 – 750 °C, depending on process duration, are presented on Fig. 4. Uncertainties were minimised by weighing three times and using average values. Transformation degree is calculated by the percentage of mass loss at given temperature and holding time to the maximum (final) weight loss from each batch, corresponding to 100% transformation into molten glass and evolution of all raw material-derived gas. The theoretical weight loss should be 2.14 wt % for Batch A and 1.91 wt % for Batch B-15 when all of the carbonates are completely

decomposed and their CO_2 evolved [22]. As shown, the transformation degree of Batch B-15 is greater than that of Batch A for any temperature or reaction time studied. The transformation degree range of silicate formation is between 25% and 80% for Batch B-15, but it is only 5% to 40% for Batch A. This indicates that the batch chemical activity is increased by introducing the briquettes. This result led to the calculation of activation energy for carbonate decomposition to provide further evidence.

3.5 Stages-of-Melting Survey

Detailed observations of the crucibles, and their cross-section specimens for Batch A and Batch B-15, shows that they reacted at different temperatures at a heating rate of 4^oC/min, as shown in Fig. 5a and 5b. All of the specimens are fractured: this cracking may be caused by the mismatch of expansion between the glass phase and batch ingredients; or the mismatch between melted batch and crucible during annealing [11]; or both. For Batch B-15, when the temperature reached 1000^oC, the shape of cubic briquette changed, consistent with melting and viscous flow. However, the boundary between briquette and other cullet is clear. Many tiny bubbles formed inside the briquette volume, which are probably due to decomposition of Na_2CO_3 in the briquette and trapping of the evolved CO_2. The shape of the cullet pieces became spherical, due in part to their relatively low viscosity at high temperature and in part to surface tension effects. Meanwhile, other refractory batch ingredients can be observed in the sample cross-sections. At 1100^oC, the briquette

was melted into glass and contained many bubbles. The shape of the briquette is distorted from its original cubic shape, and the boundary between briquette and cullet, even between different pieces of cullet, is obscured. At 1200^{o}C, the release of gas caused the fluctuating surface of the melted batch. Melted glass sinks to the bottom of the crucible and un-melted glass batch is floating on top of the melt due, it is assumed, to density / buoyancy effects. At 1300^{o}C, un-melted batch forms inclusions in the molten glass, but no layer of batch can be observed. At 1400^{o}C, only glassy phase can be observed and at 1400^{o}C for 1h, bubbles have largely disappeared.

For Batch A, the melting behaviour at 1000^{o}C and 1100^{o}C is similar to Batch B-15, except for the obvious absence of briquettes in the batch and more virgin batch components giving white powder spots, which may be the recycled filter dust. At 1200^{o}C, the surface of the glass batch is not as fluctuating as in Batch B-15. For the temperature range from 1300^{o}C to 1400^{o}C, the appearance of Batch B-15's crucible section is similar to that of Batch A.

To simulate the melting process of briquettes in glass furnaces, and to estimate the relative reaction times and rates, detailed observations of the crucibles, and their cross-section specimens showing the melting status of briquettes placed on top of the glass melt at 1450^{o}C for different times, are shown in Fig 6. To protect the mechanically-fragile tops of the samples after cooling, epoxy resin was used for sealing the samples produced after 10s, 15s, 40s, 1min and 2mins. The 1.5min sample did not require sealing.

After heating at 1450^{o}C for 10s, no obvious melting of the briquette was

observable to the eye. Under optical microscopy (not shown), a very thin melting layer formed on the upper (about 0.5mm) and lower parts (about 1.5mm) of the briquette. Meanwhile, a void forms underneath the briquette. This void may be caused by air trapped in the melt by the briquette and its expansion at high temperature, which suggests very rapid wetting between the glass melt and the briquette surface. After heating for 15s, the briquette melts, bubbles are formed inside of it, and the shape of the briquette and the void beneath it are distorted. After 40s, a cellular macrostructure formed inside of briquette from bubbles generated by the decomposition of sodium carbonate, and the void has also resolved into bubbles. After 1min, the briquette as completely melted and a layer of bubbles has formed on top of the glass melt and stuck onto the inner face of the crucible. After 5 mins, the glass melt is clarified; and no bubbles can be observed after 10 mins heating.

4. Discussion

4.1 Melting of glass batches with and without briquettes

The chemical reactions taking place during the melting of virgin soda – lime - silica glass batch were summarized in previous studies [23]. For initial melting reactions, several important reactions in the formation of the silicate melt involve the decomposition of carbonate and evolution of gas. The reactions are influenced by different raw materials and soda ash reacts with limestone at low temperatures between 450 and 650 ^{o}C to form a double bicarbonate ($Na_2Ca(CO_3)_2$) [24][25]. This double bicarbonate then reacts with silica and releases CO_2 at 900 ^{o}C; Decomposition

of carbonates including dolomite and limestone occurs in practice between 600 and 900 ^{o}C [23]. Finally, soda ash reacts with silica sand between 780 and 900 ^{o}C [15].

For virgin soda – lime - silica glass batches, carbonate decomposition temperatures occur between 600 and 900^{o}C[16]. However, the melting of soda – lime – silica glass batches with high cullet contents is quite different from pure raw material batch. In addition to the chemical reactions described above, a classical result observed by Manring and Conroy shows the selectivity of soda to react with cullet [21]. However, a trial by the same authors in an industrial furnace showed the reverse (and normally expected) behaviour: melting was accelerated by the addition of cullet, in a non-linear fashion [26]. The introduction of cullet may thus cause different reactions during melting of batch, and the sequence of the reactions can be affected by the introduction of cullet.[26]

According to the TGA and MS results for Batch A and Batch B-15, the temperature range of carbonate decomposition was 400 to 700^{o}C, which is considerably lower than that of virgin soda – lime – silica glass batch mentioned above. The introduction of cullet therefore clearly decreases carbonate decomposition temperatures. If we compare the TGA curves of Batch A and Batch B-15 shown in Fig,3, the carbonate decomposition temperature range of Batch B-15 is lower than that of Batch A with the introduction of briquette, indicating that carbonate decomposition will occur earlier in the melting process, i.e. faster. This in turn suggests a lower activation energy of decomposition upon introduction of briquettes into the batch. However, the batch samples for DTA-TGA-MS measurement were in

powder form, necessitated by the sample size acceptable for analysis with the technique. Therefore, dynamic and particle size-related influences on decomposition reactions may also be involved.

The degree of transformation of original Batch A and Batch B-15 over the temperature range 675^{o}C to 750^{o}C, are presented in Fig.4. It is clear that the degree of transformation of Batch B-15 is much greater than that of Batch A, which is consistent with the TGA-MS results. However, the degree of transformation of Batch A and Batch B-15 at 750^{o}C are 35% and 75%, respectively, even after 1h. Compared to the TGA-MS results (which indicate that the decomposition reaction is complete at 700^{o}C), this indicates that carbonate decomposition reactions in the original batch is slower than in the milled batches studied using DTA-TG-MS. The influence of particle size on the rate of reaction is therefore clear, and a fine particle size promotes the reaction by increasing the contact surface area and decreasing path lengths for material transport. In previous research, Cheng *et al.* [22] studied the decomposition kinetics of loose and granulated virgin glass batch in a similar way. the degree of transformation of glass batch before and after granulation is increased from around 20% to 40% and 20% to 60%, respectively, after 1h heat treatment at 775^{o}C. In our case, the degree of transformation of glass batch with (Batch B-15) and without (Batch A) briquettes is increased from around 45% to 70% and 20% to 35%, respectively, after 1h heat treatment at 750^{o}C. Although the heat treatment temperature in our study is lower than others, the degree of transformation of Batch A at 750^{o}C is similar to the virgin glass batch of Cheng *et al.* [22] at 775^{o}C. The increased degree of

transformation of Batch B-15 compared with Batch A, is significant. It is more than double at the beginning of the heat treatment (45%) compared to that of the granulated virgin glass batch (20%) at lower temperature, which indicates that primary decomposition of carbonate occurred at lower temperature. The main reason for this is probably that sodium carbonate was mixed and closely compressed with glass fines in the briquette, which promoted the decomposition of sodium carbonate in Batch B-15. This phenomenon cannot be determined from DTA, because for DTA the briquette was milled and mixed with other ingredients during sample preparation.

A study of decomposition kinetics was applied to the degree of transformation of Batch A and Batch B-15 to quantify their decomposition activation energies and any differences between them. The reaction rate constant was determined analytically from the Ginstling–Brounstein equation [27] which describes the kinetics of solid-phase processes in isothermal conditions (1):

$$F_{hb} = 1 - 2/3G - (1 - G)^{2/3} = K\tau \quad (1)$$

where F_{hb} is the Ginstling–Brounstein function; G is the part of a substance entered into reaction; K is the reaction rate constant; τ is reaction time. [27] Through linear fitting, the reaction rate constant K at different temperatures was obtained. All calculated values of K at different temperatures are shown in Table 3. For chemical reactions, the temperature dependence of K is given by the Arrhenius equation (2):

$$\mathrm{K} = \mathrm{A}e^{-E/RT} \rightarrow \ln K = \ln A - \frac{E}{R} \cdot \frac{1}{T} \quad (2)$$

where A, R, K, T are the pre-exponential factor, the universal gas constant, the reaction rate constant and absolute temperature, respectively. As shown in Eq. (2), ln K has a linear relationship with 1/T. The slope of this line is −E/R. The 1/T versus ln K curves of Batch A and Batch B-15 are shown in Fig. 7, according to Eq. (2). The calculated values of activation energy for carbonate decomposition are also shown in Table 4.

The activation energy for Batch A (215.56kJ/mol) is decreased to about three quarters of this value for Batch B-15 (148.94kJ/mol). Relevantly, Cheng *et al.* [22] reported the activation energy of granulated virginal glass batch decreased with increasing of binder (carboxyl methyl cellulose(CMC)) from 177kJ/mol of loose glass batch to 162kJ/mol of 0.4% CMC granulated batch. The decreasing of activation energy by introduction of briquette is substantial. Lower values of activation energy indicate, in this case, increased rates of carbonate decomposition and silicate formation [28]. Compared with the briquette-free Batch A, Batch B-15 more readily decomposes to release CO_2 and engages in fusion reactions to form silicates, at the stage of glass formation. Hrma [29] noted that the dissolution rate of silica grains during the decarbonization stage is much greater than in subsequent stages. The silicate formation and carbonate decomposition of Batch B-15 have been shown to be faster than that of Batch A, and on the basis of Hrma's [29] statement, it is conceivable that the dissolution rate of sand grains in Batch B-15 may also be greater than that of Batch A. For final melting reactions at higher temperatures, the

dissolution of sand grains in the glass melt is most important, and can be considered a diffusion controlled process [23][30].

For further study of the phase evolution and sand grain dissolution at high temperatures, Batch A and Batch B-15 were heated in the temperature range 900^{o}C to 1300^{o}C. XRD patterns are shown in Figure 1a and 1b. For both batches, Quartz (SiO_2, PDF# 05-0490) and Dolomite ($CaMg(CO_3)_2$, PDF# 05-0522) phases were identified. Other crystalline compounds such as Na_2CO_3 or $CaCO_3$ were not detected, perhaps due to their low abundance. After heat treatment at 900^{o}C, dolomite disappeared from both Batch A and Batch B-15, which indicates the decomposition of dolomite is complete at this temperature. For phase evolution, a complex low-symmetry phase $Na_4Ca_4(Si_6O_{18})$ (PDF# 75-1686) is only observed in batch A at 900^{o}C (Fig 1 c.). In addition, the formation (900^{o}C) and dissolution (1000^{o}C) of the high temperature phase wollastonite ($CaSiO_3$, PDF# 03-0626) was detected in both Batch A and Batch B-15.

The relative intensity of the diffraction peaks due to quartz (e.g. at $2\theta=26.74^{o}$) decreases with increasing temperature. From 1100^{o}C to 1300^{o}C, the only crystalline phase present in both Batch A and Batch B-15 was quartz, with the broad amorphous hump indicating that the remainder of the samples were X-ray amorphous. Most importantly, the relative intensity of the main quartz reflection at $2\theta=26.74^{o}$ is not present in the sample heated to 1200^{o}C for Batch B-15, whereas it is present for Batch A, and has only disappeared in the sample heated to 1300^{o}C. This indicates that the dissolution of sand grains in Batch B-15 occurs at lower temperatures / is more rapid

than in Batch A. Whilst the proportion of sand in Batch B-15 is indeed lower than that in Batch A, this behaviour is consistent with the promotion of decomposition of carbonate raw materials at lower temperatures in Batch B-15 compared with Batch A.

Dolan and Misture carried out a series of accurate in-situ XRD studies on binary and ternary soda-lime-silica glass batch components reactions with and without cullet [13]. For laboratory (66 wt% quartz–33 wt% sodium carbonate) batch that was heated to 1200^{o}C, Na_2SiO_5 was identified from 600-900^{o}C and Na_2SiO_3 was identified from 650-1000^{o}C. For laboratory (66 wt% quartz-17 wt% sodium carbonate-17wt% calcium carbonate) batch that was heated to 1200^{o}C, the observed was more complicated: $CaCO_3$ and Na_2CO_3 disappeared before 800^{o}C and 900^{o}C respectively; $Na_2Si_2O_5$ was identified from 700-800^{o}C; Na_2SiO_3 was identified from 650-1100^{o}C; $Na_2Ca_2Si_3O_9$ was identified from 800-1100^{o}C; $Na_4CaSi_3O_9$ was identified from 840-1200^{o}C; Ca_2SiO_4 was identified from 800-1200^{o}C; $CaSiO_3$ was identified from 1000^{o}C to 1200^{o}C; and quartz was identified at all temperature ranges. For cullet containing batch, Dolan and Misture [13] also studied 50 wt% cullet-50 wt% (66 wt% quartz-33 wt% sodium carbonate) batch heated at 775^{o}C for different times. Quartz, $Na_4CaSi_3O_9$, $Na_2Si_2O_5$ and Na_2SiO_3 were identified. For industrial float glass batch with cullet removed, and heated to 1200^{o}C, $Na_4CaSi_3O_9$ and $Na_2Ca_2Si_3O_9$ were identified.

By comparison, in our reacted glass batch, $CaSiO_3$, SiO_2 and $Na_4Ca_4(Si_6O_{18})$ were identified. For $CaSiO_3$ and SiO_2 this is consistent with Dolan and Misture's results. In figure 1c, the identification of $Na_4Ca_4(Si_6O_{18})$ is unique but not unexpected:

for example, Dolan and Misture also found several complex low-symmetry phases such as $Na_4CaSi_3O_9$ and $Na_2Ca_2Si_3O_9$ as described above. Glass batch components are almost chemically independent (such as SiO_2, Na_2CO_3 and $CaCO_3$, no pre-existing chemical bonds between the silicate network and calcium/sodium raw materials except cullet). The formation and transformation of polysilicate from these components arise through the melting process of glass batch. On a local chemical level, due to the multiple sources of batch component and particle-particle interactions, the reaction path may follow different route (although a uniform glass phase is finally formed). The identification of these phases by XRD offers us an intriguing glimpse into the formation and transformation of polysilicates. It is also consistent with the weak DTA signals in the high temperature range, detected after the decomposition of carbonate.

In summary, this subset of experiments has confirmed that introduction of briquettes to the batches studied here increases the rate of the reaction during batch melting. It promotes batch melting behaviour such as decomposition of carbonates, formation of silicates and dissolution of sand at lower temperatures. The decrease in activation energy results in an increase in melting rate.

4.2 Section survey and Briquette melting behaviour

Glass batches are complex mixtures of chemically and physically different raw materials. Consequently, melting behaviour or processes during heating are highly complex and challenging to evaluate through a single indicator. To study the melting

process of glass batches visually, a stages-of-melting survey of cross-sectioned crucibles containing samples of Batch A and Batch B-15, a heat treatment was applied to different temperatures at a heating rate of 4^{o}C/min. This enabled direct, qualitative, macroscopic assessment and comparison of batch reactions, sintering and shrinkage during melting. It also enabled evaluation of melting defects such as solid inclusions, bubbles and chemical inhomogeneities, which are intimately associated with the quality of glass products.

Before heat treatment, briquette cubes were buried within the batch, approximately 2 to 3mm above the bottom of the crucible. As shown in Figure 5b, at 1000^{o}C, the briquette cube melted and began to flow; and consequently it lost its original shape. At 1000^{o}C, cullet particles remain separated and have clear boundaries between each other, with other ingredients interspersed in the cross-section. This is observed for both Batch A and Batch B-15 in Fig. 5 a and b. It is also observed that the briquette melted before the surrounding cullet, and before the other batch ingredients are converted. At 1100^{o}C, the cullet in both Batch A and Batch B-15 has all melted. No obvious voids between distorted cullet particles can be observed, and melted cullet particles adhere together and can be observed due to their different colours. Although the raw materials are different, this lack of homogeneity of glass melting in the crucible was observed and characterized by the occurrence of layers of different chemical composition and density [31]. This behaviour was believed to be due to kinetic factors such as elemental distributions and grain size distributions of the raw materials.[31] At 1100^{o}C the briquette in Batch B-15 has completely melted and

transformed into glass phase with high bubble content. Interestingly, the top surface of batch B-15 melt is indented, suggesting wetting between the glass melt and the inner wall of the Al_2O_3 crucible, which is related to the surface tension of the liquid phase. Meanwhile the surface of Batch A is still uneven. This suggests that more liquid phase is present in Batch B-15 at 1100^{o}C. Also it is noted that the position of the melted briquette moves upwards in the crucible due to buoyancy effects and, in so doing, provide physical agitation of the batch / melt mixture. At 1200^{o}C, the top surface of Batch B-15 fluctuates, probably due to gas evolution. For batch A, the top surface is indented with no fluctuations, which suggests the reaction or the melting process in batch A lags behind Batch B-15 again. At 1300^{o}C, both of Batch A and Batch B-15 were melted, with bubbles and solid inclusions also present. At 1400^{o}C, only a few bubbles can be observed in the cross section; and both glass melts were clarified at 1400^{o}C after 1h of heating.

Other aspects requiring consideration are the melting behaviour of briquettes and their reaction with molten glass, and whether briquettes are wetted by the molten glass. In commercial glass manufacturing, batch piles or blankets float on the surface of the molten glass because the bulk density of the batch is usually about one-half that of the glass melt [8]. Yet 65% - 75% of the melting reactions occur on the top surface of the batch pile or blanket in a fuel-fired furnace [8]. As a novel batch component, we need to study the melting process of briquettes when floating on the surface of the molten glass. To simulate such processes in a laboratory glass furnace, 9 cubes made from briquettes were placed on the top of the molten glass, which was pre-melted contained

in small crucibles and heated at 1450^{o}C for different times. All crucibles were cooled and cross-sectioned, with surveys presented in Fig.6.

In this part of our study small crucibles, rather than larger ones, were selected as they enabled all experiments to be carried out in one furnace during the same period, minimising experimental variability. There may be some effect of other batch components potentially changing the local chemistry around the briquettes, owing to the large size of briquettes relative to crucible volumes. However, the most important research questions here - an accurate assessment of how the briquette will melt under such conditions, and the wetting capability of the briquettes and the batch / melt - were answered satisfactorily. Moreover, briquette compositions are similar to the glass melt, which could be approximated. [6] Larger crucible studies may provide additional useful information, and are suggested as further work, however, they may also introduce new variable parameters since accurate reproduction of melting conditions will be more challenging on a melt-by-melt basis.

As described earlier, the briquette cube always floats on the surface of molten glass. Briquette melting was complete within just 1 minute. During melting, a cushion was formed underneath of the briquette for the sealed air and its expansion. The venting of the air from the cushion may also help to stir the melt, although further work is required to confirm this.

5. Conclusions

Briquettes made from cullet fine particles, sodium silicate, sodium carbonate and water were introduced at 15 wt % into a representative green container glass batch and their melting behavior compared with that of a briquette-free batch. TGA-MS showed that the carbonate decomposition temperature of the batch with briquette addition (Batch B-15) ranged from ca. 400^{o}C to 680^{o}C, lower than that of the briquette-free Batch A (ca. 600^{o}C to 900^{o}C). The decomposition temperature of Batch B-15 is lower than that of Batch A. Batches A and B-15 were treated at temperatures of 675-750^{o}C for different times, and demonstrated that the degree of transformation of Batch B-15 and Batch A differ. For Batch A, the degree of transformation varies from 5% to 35%; and for Batch B-15, it varies from 25% to 75%. The calculated carbonate decomposition activation energy for Batch A (215.56 kJ/mol) is decreased to about three quarters of that of Batch B-15 (148.94 kJ/mol). It also indicated that the introduction of briquette accelerates the decomposition of carbonate and the formation of silicate. From XRD, the phase transitions of Batch A and Batch B-15 during melting are similar: wollastonite was present from 1000^{o}C to 1200^{o}C; whilst quartz had totally melted at 1200^{o}C for Batch B-15 and 1300^{o}C for Batch A. The batch and briquette melting behaviour at different temperatures was directly observed through a crucible section survey. Melting of briquettes occurs ahead of cullet and other batch ingredients at lower temperatures. Introduction of briquettes promotes the presence of liquid phases and convection in the batch. An effervescent melting process was observed when a briquette was placed on top of the molten glass at 1450^{o}C.

Acknowledgements

The authors acknowledge financial support from EPSRC under grant EP/P510725/1 and Innovate UK under grant 63406-429275. The authors appreciate useful discussions with Vincenzo Starinieri, Francis Clegg, Anthony Bell, Paul Allender, Tim O'Hara, Leo Olowookere and James Burke.

References

[1] Ruth M, Dell'Anno P. An industrial ecology of the US glass industry. Resour Policy. 1997; 23: 109–124.

[2] Deng W, Cheng J-S, Deng Z-L, Deng M. Research of Sintering Reactions Process and heat Calculation in Glass batch. J Wuhan Univ Technol. 2010; 22: 111–113.

[3] Bingham PA, Hyatt NC, Hand RJ. Vitrification of UK intermediate level radioactive wastes arising from site decommissioning: Property modelling and selection of candidate host glass compositions, Glas Technol Eur J Glas Sci Technol Part A. 2012; 53: 83–100.

[4] Bingham PA, Marshall M. Reformulation of container glasses for environmental benefit through lower melting temperatures. Glas. Technol. 2005; 46: 11–19.

[5] Kovacec M, Pilipovic A, Stefanic N. Impact of glass cullet on the consumption of energy and environment in the production of glass packaging material. Recent Res Chem Biol Environ and Cult. Monteux, Switzerland. 2011.

[6] Deng W, Wright R, Boden-Hook C, Bingham PA. Briquetting of recycled glass cullet fine particles for energy-saving glass manufacture. Glas Technol Eur J Glas Sci Technol Part A. 2018; 59: 81-91.

[7] Beerkens R. Modular melting-Industrial Glass melting process requirements Part 2. Am Ceram Soc Bull. 2004; 83: 35–38.

[8] Bauer WC, Bailey JE. Raw materials/batching. Engineered Materials Handbook: Vol 4 Ceramics and glasses. ASM International. 1992.

[9] Beerkens R, Kers G, Santen EV, Recycling of Post-Consumer Glass: Energy Savings, CO_2 Emission Reduction, Effects on Glass Quality and Glass Melting, 71st Conf Glas Probl. John Wiley & Sons. 2011: 167–194.

[10] Bunting JA, Bieler BH. Batch Free Time Versus Crucible Volume in Glass Melting. Am Ceram Soc Bull. 1969; 48: 781–785.

[11] Bieler BH, Bunting JA. Batch-free time vs Crucible volume and soda Type in Glass melting. Am Ceram Soc Bull. 1984; 63: 1405–1407.

[12] Dolan MD, Misture ST. Analysis of glass batch reactions using in-situ x-ray diffraction. Part I. Borosilicate glass batches. Glas Technol. 2004; 45: 140–147.

[13] Dolan MD, Misture ST. Analysis of glass batch reactions using in-situ x-ray diffraction. Part II. Borosilicate glass batches, Glas Technol. 2004; 45: 167–174.

[14] Dolan MD, Misture ST. Analysis of glass batch reactions using in-situ x-ray diffraction. Part III. Borosilicate glass batches, Glas Technol. 2004; 45: 212–219.

[15] Hong KS, Speyer RF. Thermal Analysis of Reactions in Soda-Lime Silicate Glass Batches Containing Melting Accelerants: I, One- and Two-Component Systems. J Am Ceram Soc. 1993; 76: 598–604.

[16] Hong KS, Lee SW, Speyer RF. Thermal Analysis of Reactions in Soda–Lime Silicate Glass Batches Containing Melting Accelerants: II, Multicomponent Systems. J Am Ceram Soc. 1993; 76: 605–608.

[17] Cheng J-S, Deng Z-L, Du X. Decomposition properties of granulated glass batch, Glas Technol Eur J Glas Sci Technol Part A. 2013; 54: 141–146.

[18] Wallenberger, Frederick T, Bingham PA. Fiberglass and glass technology : energy-friendly compositions and applications. Springer, 2009.

[19] Mukerji J, Nandi AK, Sharma KD. Reaction in Container Glass Batch. Am Ceram Soc Bull. 1980; 59: 790–793.

[20] Manring WH, Bauer WC. Influence of Batch Preparation Process on the Melting and Fining of Glass. Glas Ind. 1964; 45: 354–357.

[21] Manring WH, Conroy AR. Influence of Cullet in the melting of soda-lime glasses. Glas Ind. 1968; 49: 269–270.

[22] Cheng J-S, Deng Z-L. Decomposition kinetics of granulated glass batch. J Non Cryst Solids. 2012; 358; 3294–3298.

[23] Marson P, Beerkens R, Rongen M. Observation of Batch Melting and Glass Melt Fining and Evolved Gas Analysis. 74th Conf Glas Probl. John Wiley & Sons, Inc. 2014; 69–80.

[24] Montoya BG, Torres-Martínez LM, Quintana P, Ibarra J. Alternative batch compositions in the glass-forming region of the Na_2O-CaO-SiO_2 system. J Non Cryst Solids. 2003; 329; 22–26.

[25] Meechoowas E, Ketboonruang P, Tapasa K, Jitwatcharakomol T. Improve melting glass efficiency by Batch-to melt conversion, Procedia Eng. 2012; 32: 956–961.

[26] Loredo JR, Martinez A, Becerril B. Cullet as a substitute for soda. J Non Cryst Solids. 1986; 84 : 414–420.

[27] GIESS EA. Equations and Tables for Analyzing Solid- state Reaction Kinetics. J Am Ceram Soc. 1963; 46: 374–376.

[28] Krasheninnikova NS, Frolova IV, Vereshchagin VI. Application of Granulated Raw Concentrate in Glass Technology. Glas Ceram. 2004; 61: 164–167.

[29] Hrma P. Reaction between Sodium Carbonate and Silica Sand at 874°C < T < 1022°C. J Am Ceram Soc. 1985; 68: 337-341.

[30] Zhao Y, Yin H. Glass Technology. Chemical Industry Press. Beijing. 2006.

[31] Chopinet MH, Gouillart E, Papin S, Toplis MJ. Influence of limestone grain size on glass homogeneity. Glas Technol Eur J Glas Sci Technol Part A. 2010; 51: 116–122.

Figures

Figure 1: a) X-ray diffraction measurements for the reacted glass batch – Batch A at different temperature, heated at 4^{o}C/min; b) X-ray diffraction measurements for the reacted glass batch, Batch B-15, at different temperature, heated at 4^{o}C/min; c) The XRD identification of Batch A, which heat treated at 900 ^{o}C. *(D: Dolomite, PDF#: 05-0622; W: Wollastonite, PDF#: 03-0626; Q: Quartz, PDF#: 46-1045; C: $Na_4Ca_4(Si_6O_{18})$, PDF#: 75-1686)*

Figure 2: a) DTA-TGA-MS analysis of Batch A; b) DTA-TGA-MS analysis of Batch B-15.

Figure 3: Normalized TGA curves for Batch A and Batch B-15 from 300^{o}C to 800^{o}C.

Figure 4: Transformation degree of Batch A (in round dots) and Batch B-15 (in triangle dots) in the heating range 675^{o}C to 750^{o}C.

Figure 5: Crucible containing melting section survey of Batch B-15 and Batch A heated to different temperatures at a heating rate of 4^{o}C/min.

Figure 6: Melting of briquettes placed on top of the glass melt at 1450^{o}C for different times.

Figure 7: a) Reaction time versus 1-2/3G-$(1-G)^{2/3}$ plots of Batch A and Batch B-15 after heating at 725^{o}C for different times. b) 1/T versus lnK plots of Batch A and Batch B-15.

Table 1. Batch compositions of Batch A and Batch B-15

	Batch A wt. %	Batch B-15 wt. %
Sand	6.61	5.91
Soda ash	1.15	0.01
Limestone	0.37	0.36
Dolomite	2.67	2.64
Chrome premix *	0.95	0.94
Na_2SO_4	0.14	0.14
Manganese ore *	0.18	0.18
Filter dust ‡	0.46	0.45
Cullet	87.47	74.47
Briquette	0	14.9
Total	100.00	100.00

* Tailings from mineral companies; ‡ Flue gas filter dust.

Table 2. XRF analyses of Batch A and Batch B-15 glass samples (wt. %)

	Nominal composition	Batch A	Error (±)	Batch B-15	Error (±)
Na_2O	13.5	13.24	0.10	13.53	0.1
MgO	1.95	1.97	0.02	1.98	0.03
Al_2O_3	1.82	2.78	0.10	2.85	0.1
SiO_2	71	69.53	0.20	70.07	0.2
K_2O	0.84	1.10	0.07	0.85	0.003
CaO	9.92	9.89	0.20	9.32	0.01
Cr_2O_3	0.34	0.38	0.01	0.38	0.04
MnO	0.16	0.18	0.01	0.18	0.01
Fe_2O_3	0.47	0.57	0.01	0.53	0.007
SO_3	\	0.09	0.00	0.08	0.004
P_2O_5	\	\	\	\	\
TiO_2	\	0.09	0.02	\	\
SrO	\	0.11	0.00	0.10	0.01
BaO	\	0.07	0.00	0.07	0.001
Cl	\	\	\	0.06	0.001
PbO	\	\	\	\	\
Total	100.00	100.00	\	100.00	\

Table 3. Reaction rate constant, K, at different temperatures.

Temperature (^{o}C/K)	K of Batch A	K of Batch B-15
675/ 948	3.82E-05 ± 3.50E-06	1.97E-04 ± 4.94E-05
700/ 973	1.14E-04 ± 1.80E-05	4.64E-04 ± 2.90E-05
725/998	2.10E-04 ± 2.30E-05	5.88E-04 ± 2.48E-05
750/ 1023	2.85E-04 ± 9.02E-05	1.64E-03 ± 1.11E-04

Table 4. Calculated activation energy, E_a for decomposition of carbonate in Batch A and Batch B-15.

	Batch A	Batch B-15
E_a (kJ/mol)	215.6	148.9
Standard Error	36.9	35.2

a)

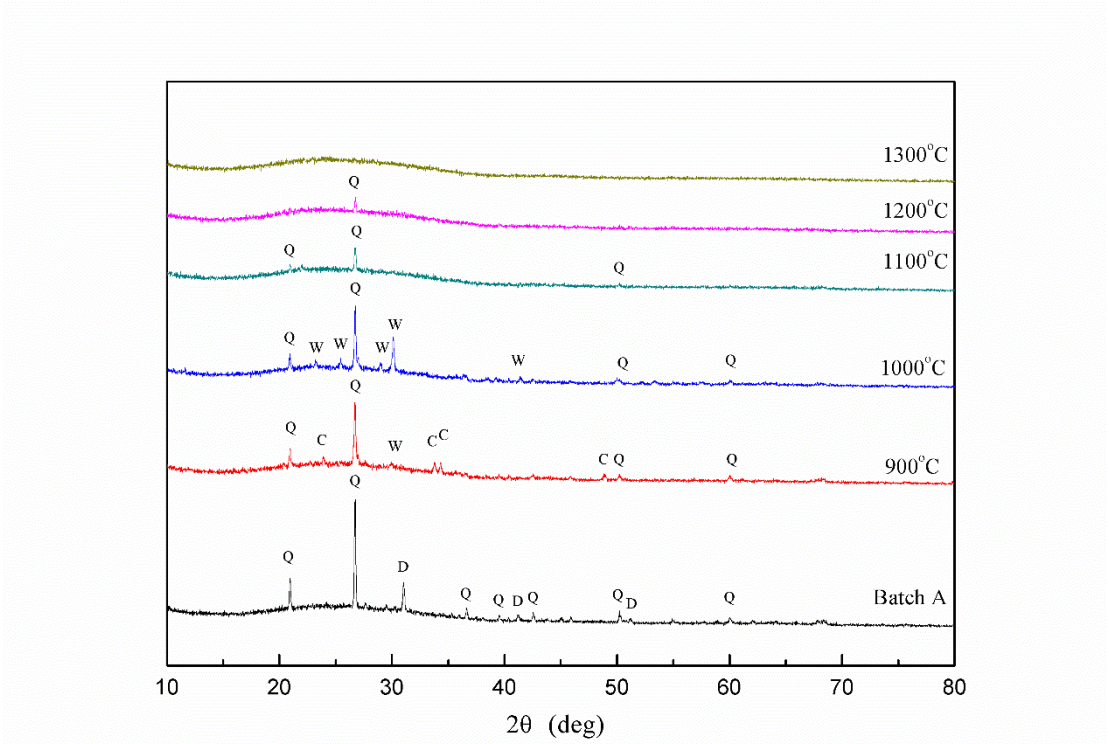
1300°C
1200°C
1100°C
1000°C
900°C
Batch A
10
20
30
40
50
60
70
80
2θ (deg)

b)

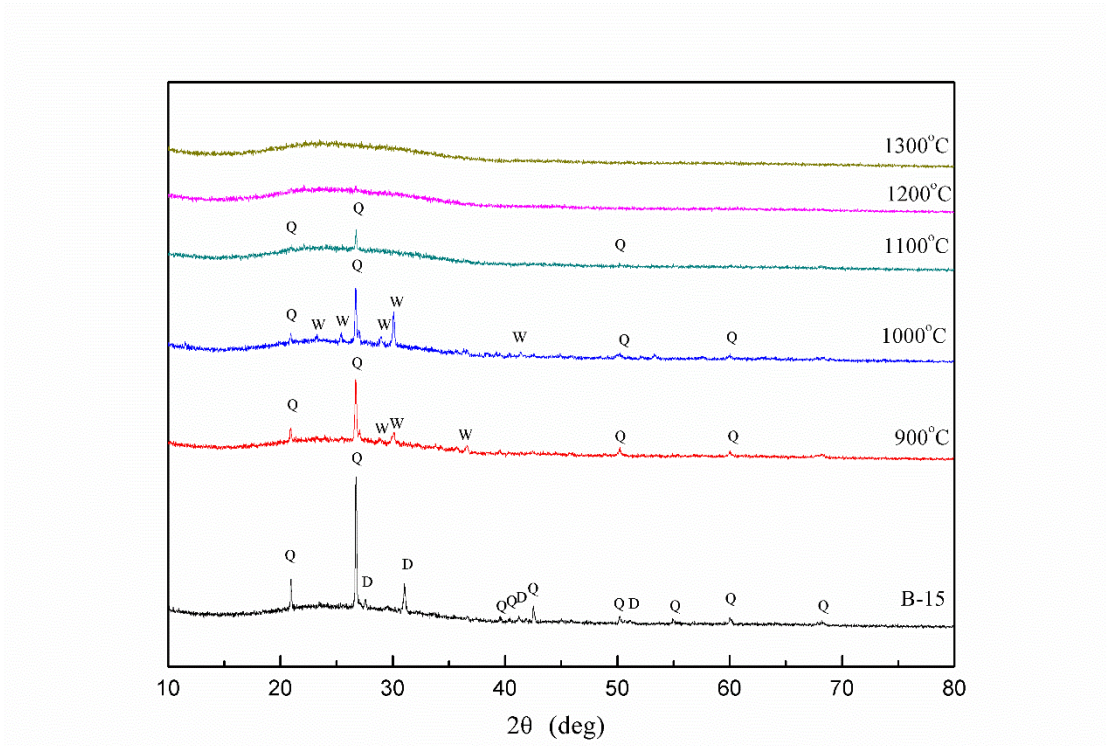
1300°C
1200°C
1100°C
1000°C
900°C
B-15
10
20
30
40
50
60
70
80
2θ (deg)

c)

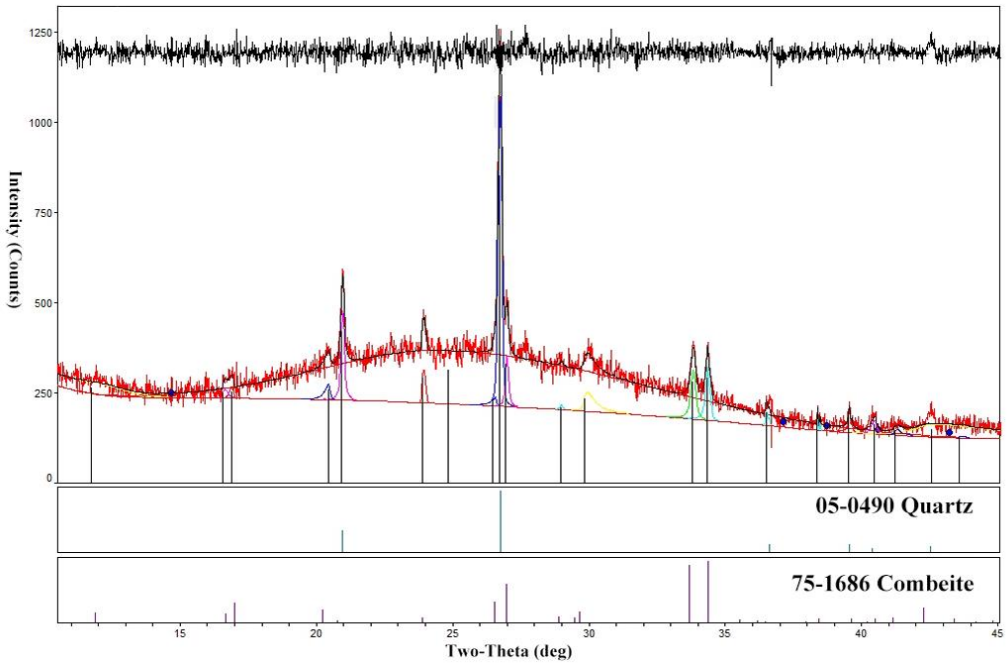

Figure 1. a) X-ray diffraction measurements for the reacted glass batch – Batch A at different temperature, heated at 4^{o}C/min; b) X-ray diffraction measurements for the reacted glass batch, Batch B-15, at different temperature, heated at 4^{o}C/min; c) The XRD identification of Batch A, which heat treated at 900 ^{o}C. *(D: Dolomite, PDF#: 05-0622; W: Wollastonite, PDF#: 03-0626; Q: Quartz, PDF#: 46-1045; C: $Na_4Ca_4(Si_6O_{18})$, PDF#: 75-1686)*

a)

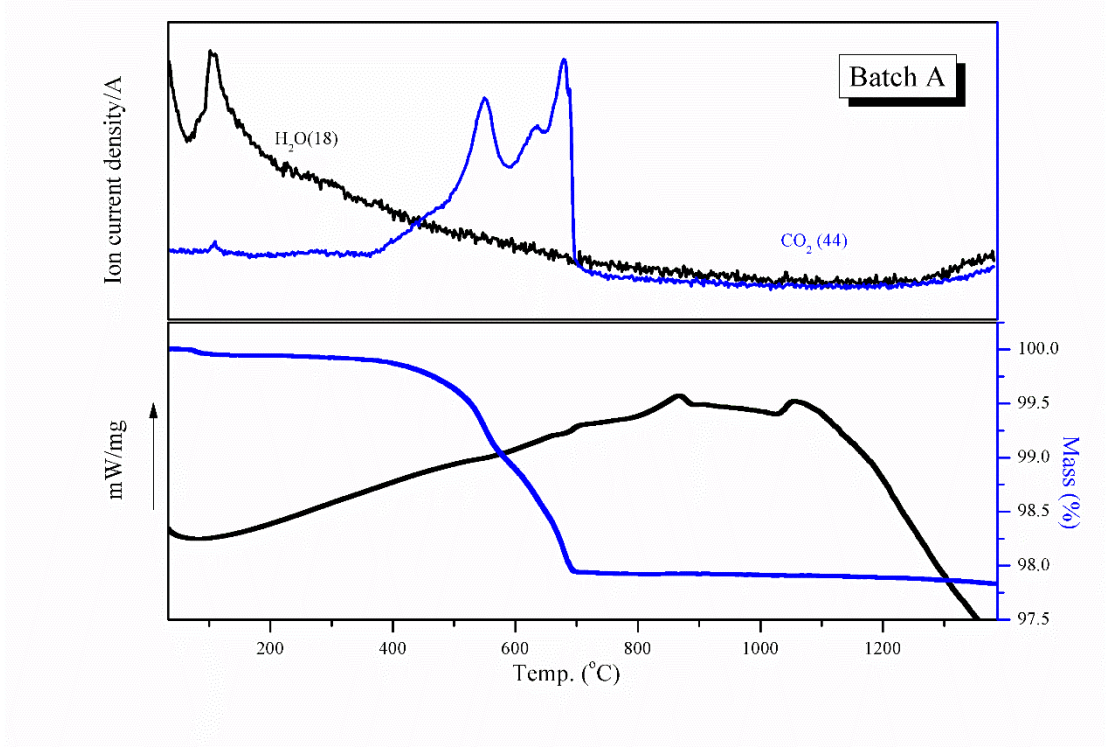

b)

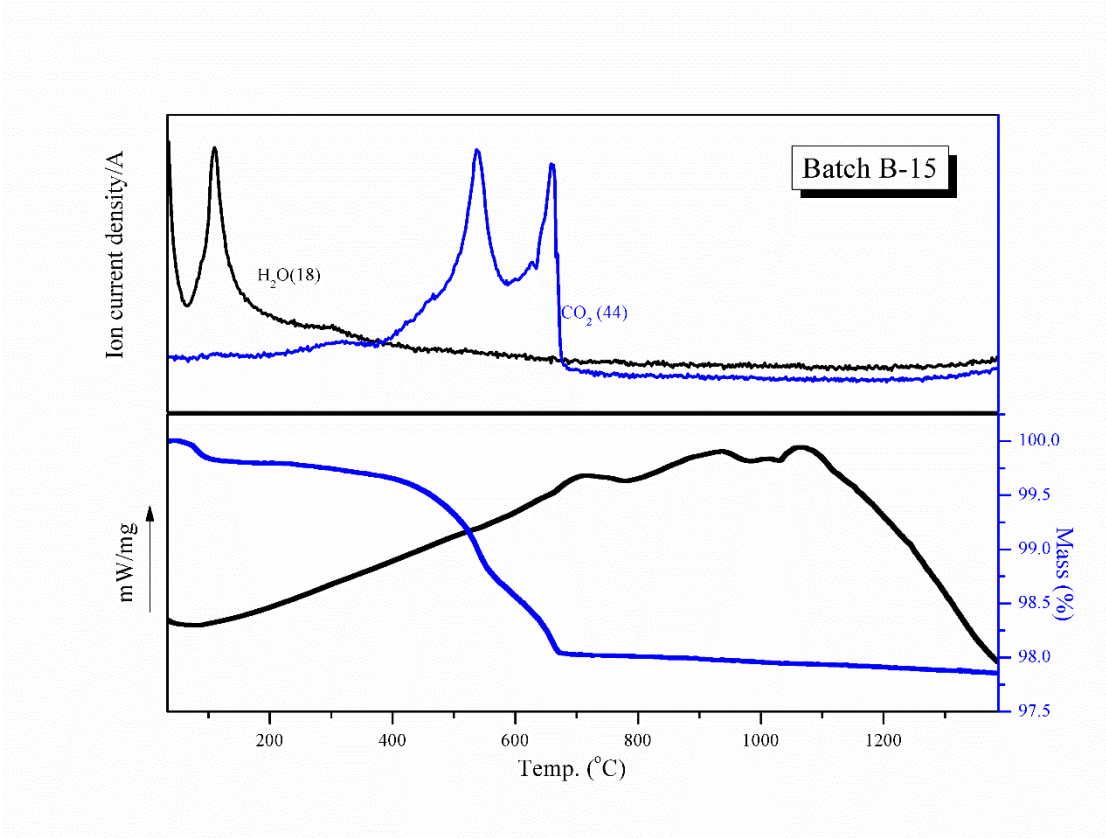

Figure 2. a) DTA-TGA-MS analysis of Batch A; b) DTA-TGA-MS analysis of Batch B-15.

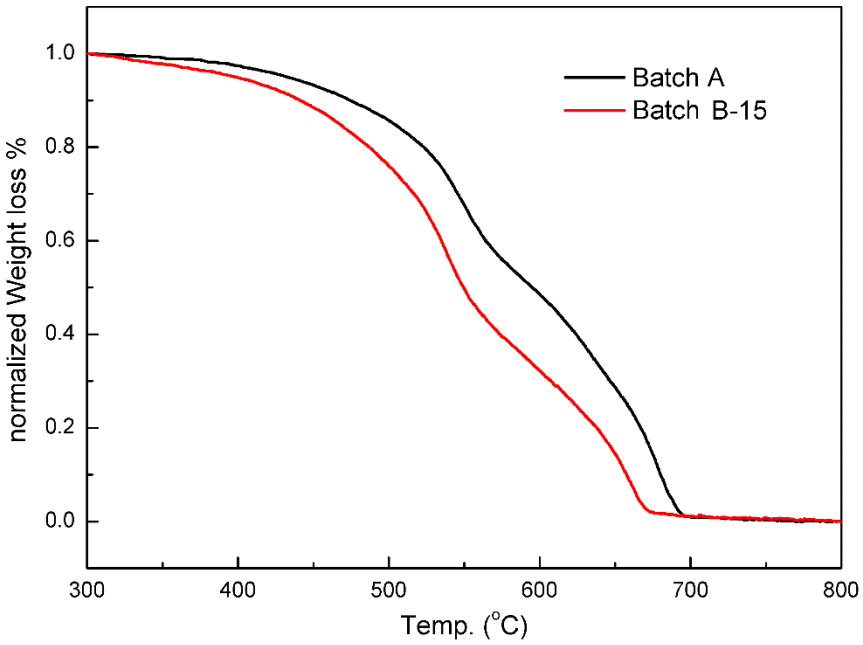

Figure 3. Normalized TGA curves for Batch A and Batch B-15 from 300°C to 800°C.

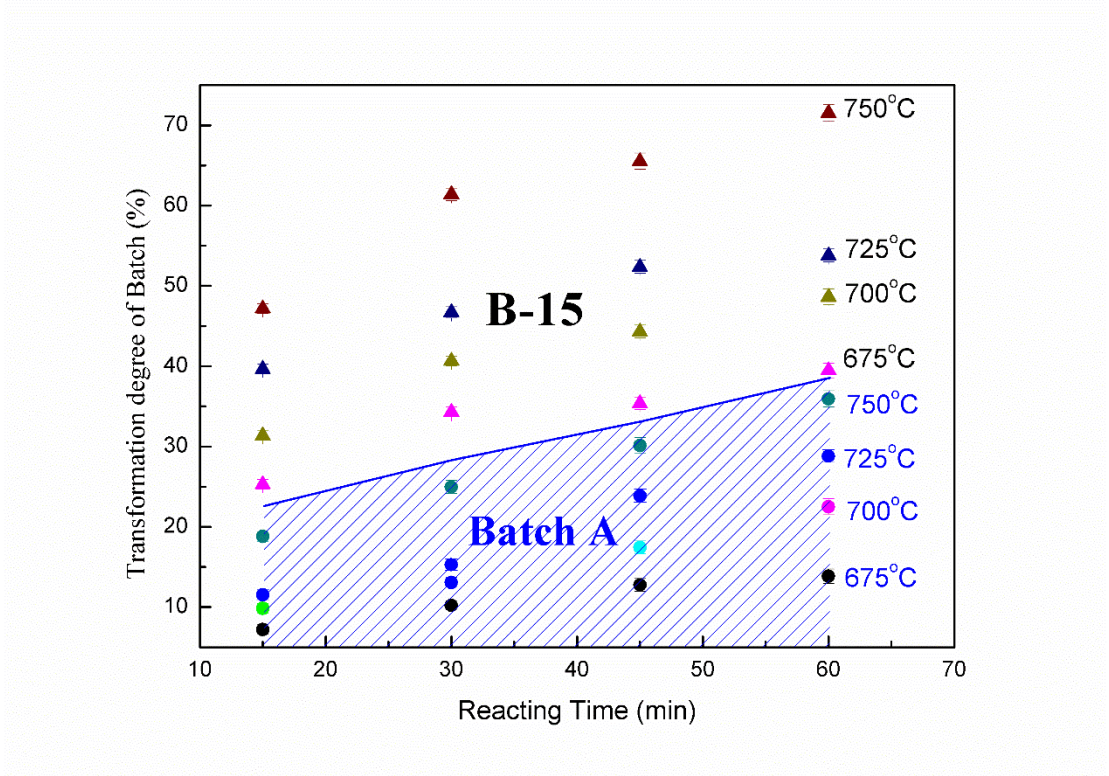

Figure 4. Transformation degree of Batch A (in round dots) and Batch B-15 (in triangle dots) in the heating range 675°C to 750°C.

a) Batch A

1000°C

1100 °C

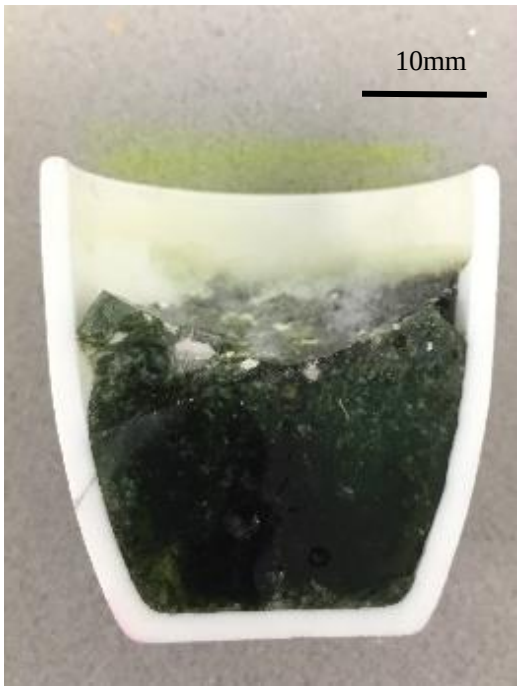

1200 °C

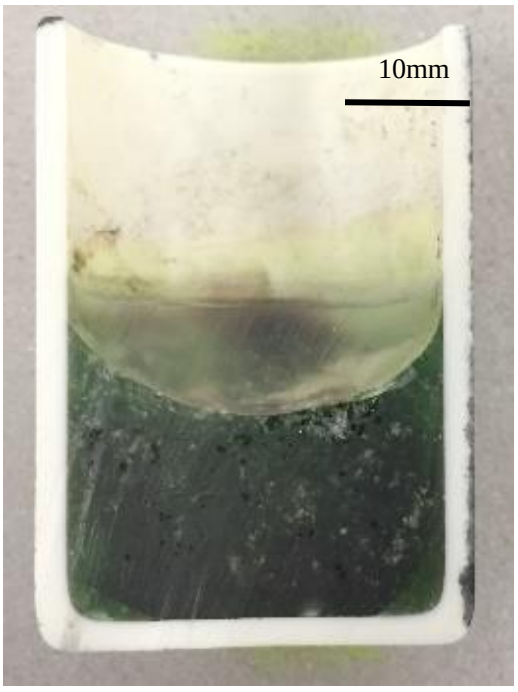

1300 °C

1400 °C

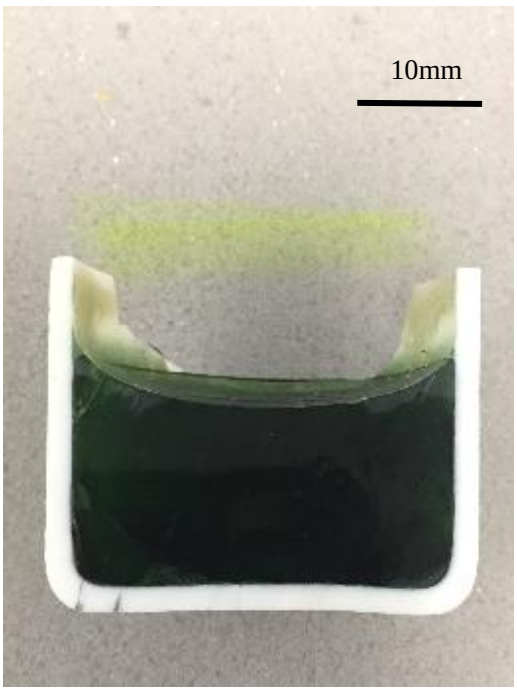

1400 °C for 1h

b) Batch B-15

1000°C

1100 °C

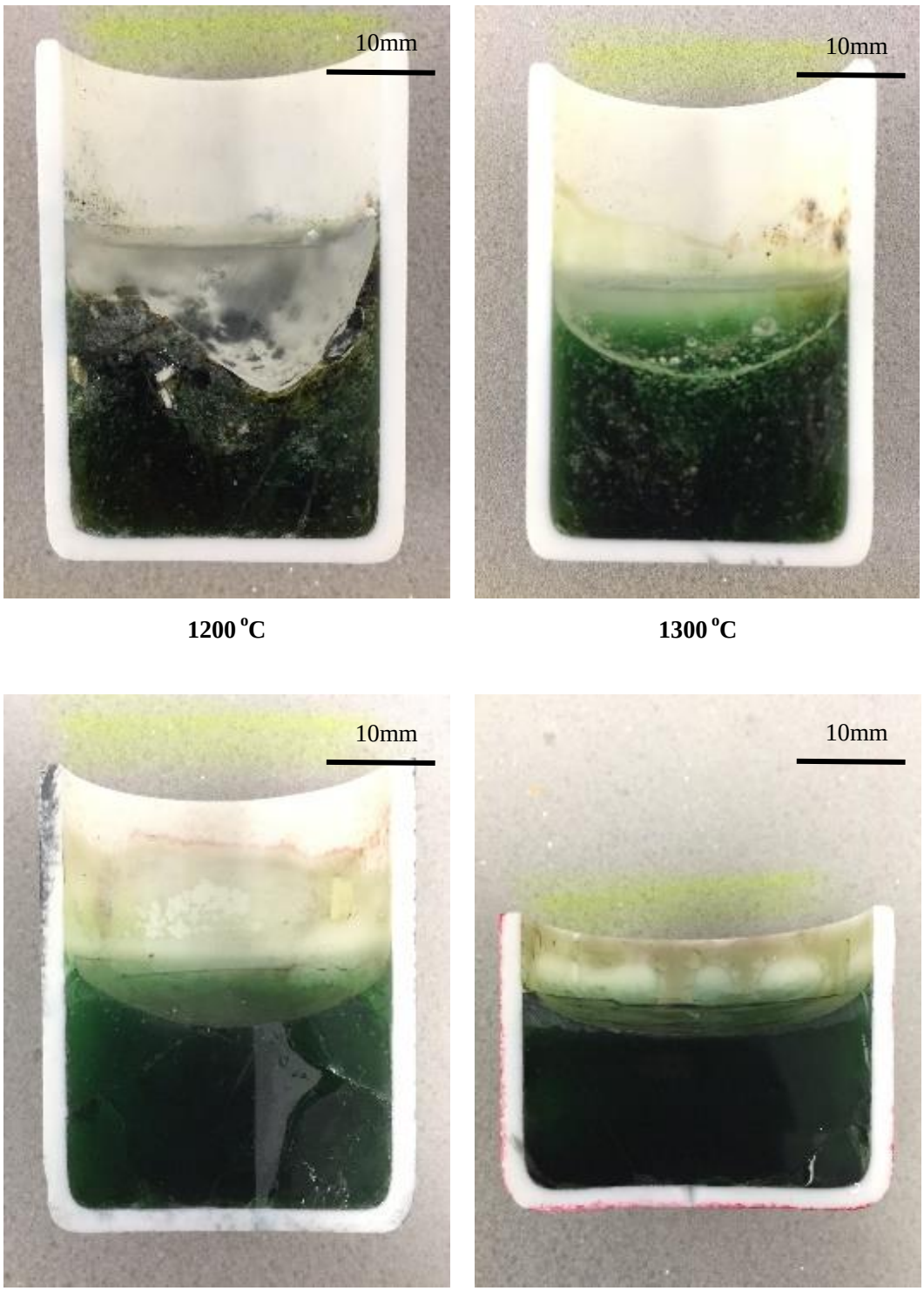

1200 °C **1300 °C**

1400 °C **1400°C for 1h**

Figure 5. Crucible containing melting section survey of Batch B-15 and Batch A heated to different temperatures at a heating rate of 4°C/min.

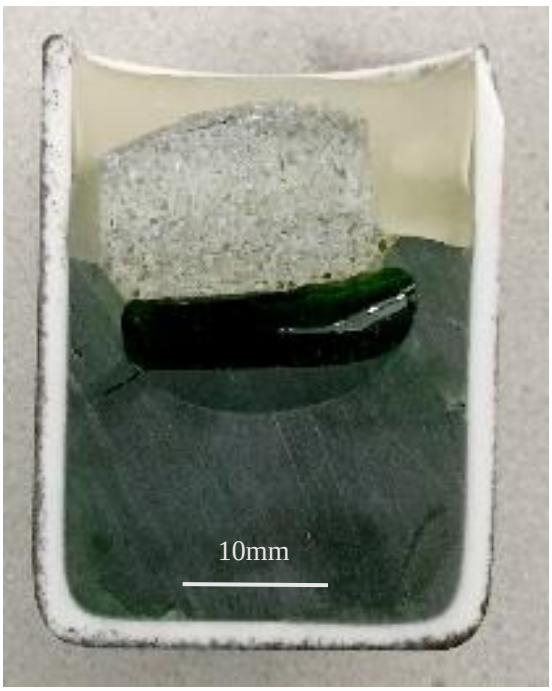

10 s

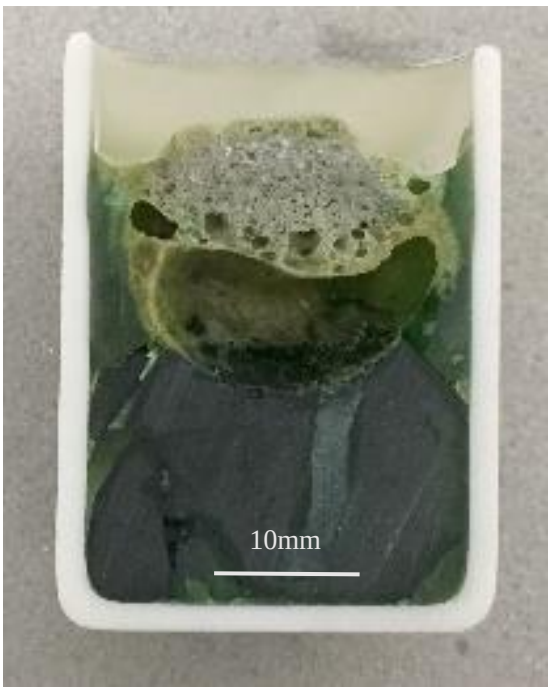

15 s

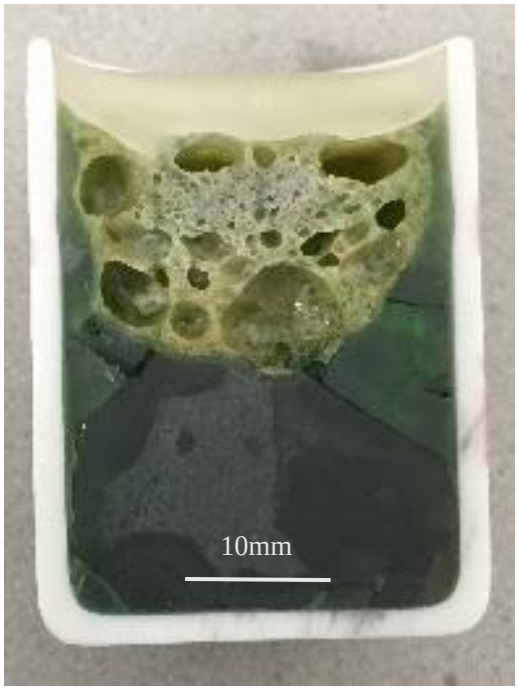

40 s

1 min

1.5 mins

2 mins

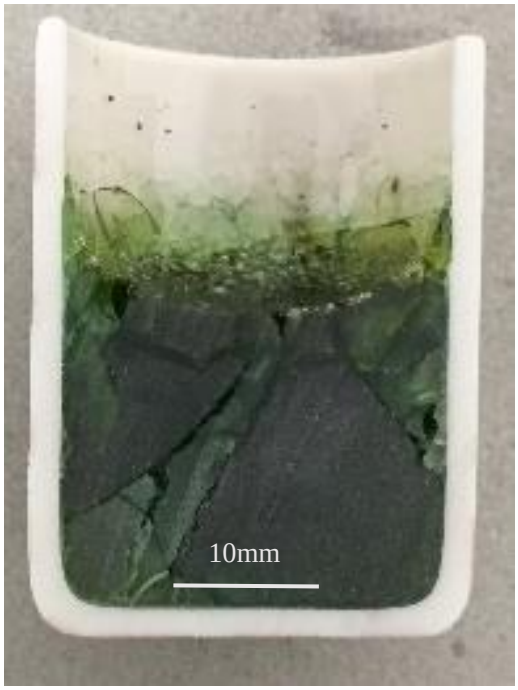

3 mins

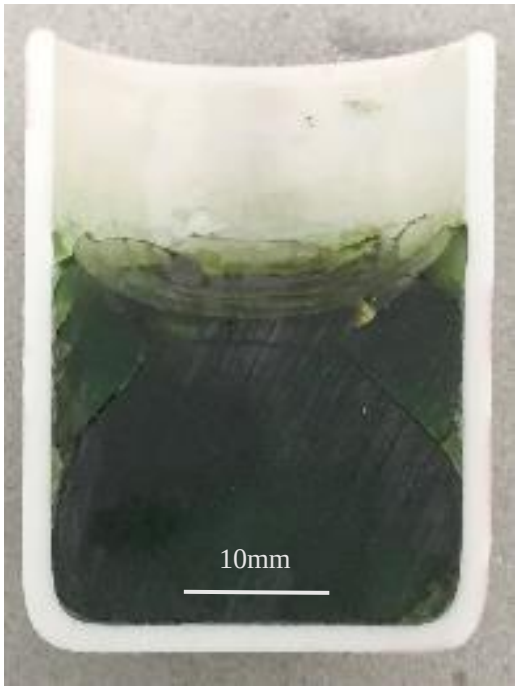

5 mins

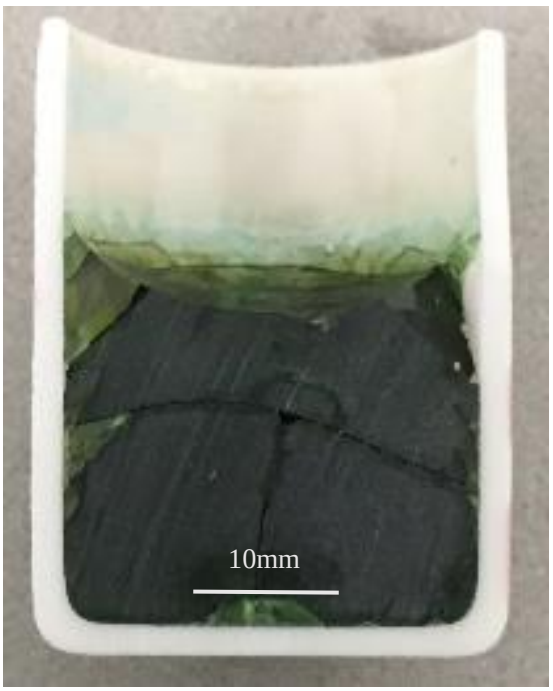

10 mins

Figure 6. Melting of briquettes placed on top of the glass melt at 1450^{o}C for different times.

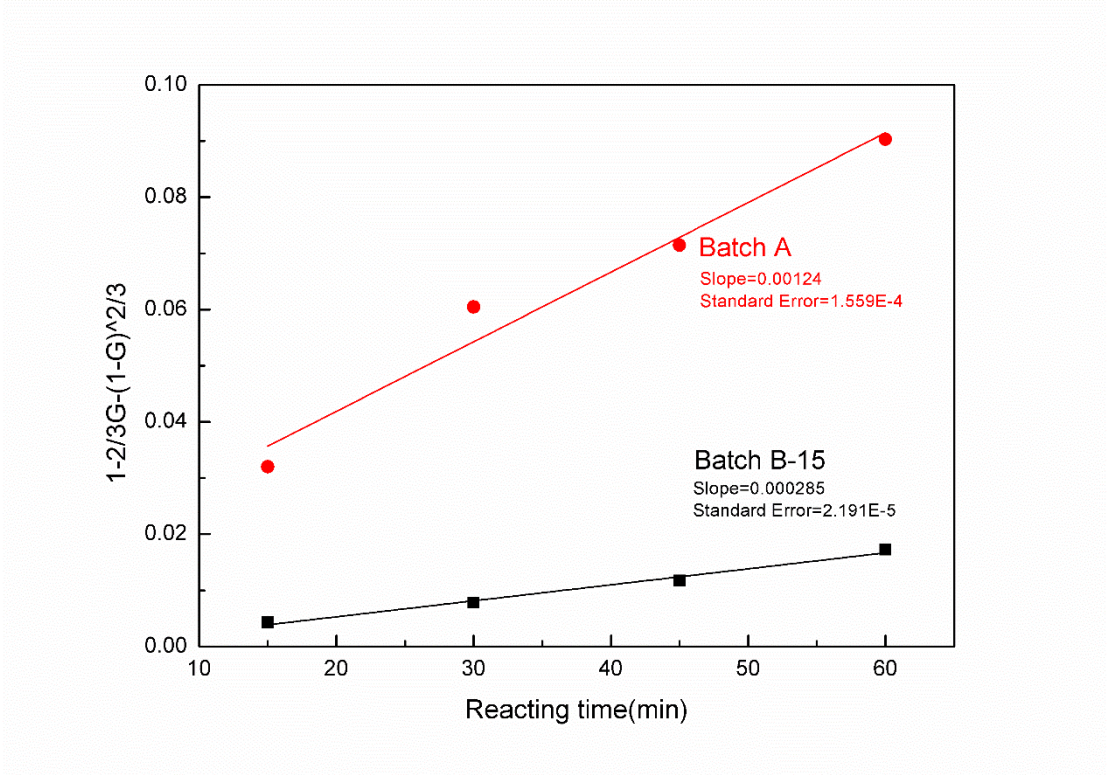

b

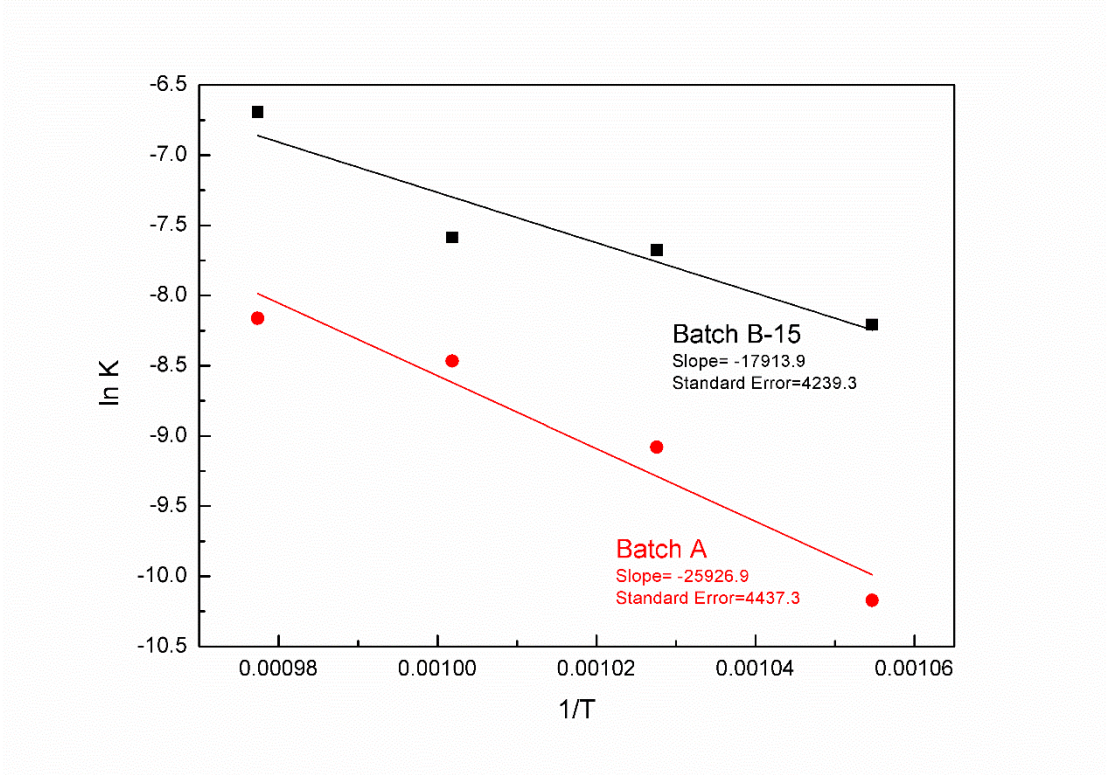

Figure 7. a) Reaction time versus 1-2/3G-$(1-G)^{2/3}$ plots of Batch A and Batch B-15 after heating at 725^{o}C for different times. b) 1/T versus lnK plots of Batch A and Batch B-15.